JCTC Journal of Chemical Theory and Computation

# Origins of Rotational Barriers in Hydrogen Peroxide and Hydrazine

Lingchun Song,[†] Minghong Liu,[‡] Wei Wu,[†] Qianer Zhang,[†] and Yirong Mo*[,†,‡]

*Department of Chemistry, State Key Laboratory for Physical Chemistry of Solid Surfaces, Center for Theoretical Chemistry, Xiamen University, Xiamen, Fujian 361005, P. R. China, and Department of Chemistry, Western Michigan University, Kalamazoo, Michigan 49008*

Received December 21, 2004

**Abstract:** Compared with their isoelectronic system ethane, both hydrogen peroxide and hydrazine exhibit a double well torsional energy curve where skew conformers are favored over trans conformers and cis conformers are energy-maximum states. Clearly, the involvement of the lone oxygen and nitrogen pairs, or more specifically, the enhanced stabilizing n→$\sigma$* negative hyperconjugation effect and destabilizing repulsion among lone pairs, complicates the conformational analysis. In this work, the modern ab initio valence bond (VB) method is employed to quantitatively investigate the torsional energy curves of hydrogen peroxide and hydrazine in terms of hyperconjugative stabilization, steric repulsion, and structural and electronic relaxations. It is found that if the hyperconjugation effect is completely quenched, the trans conformers will be favored, while the cis conformers are the only transition state pertaining to the torsional motion in the potential energy surfaces of $H_2O_2$ and $N_2H_4$. Although usually the steric effect includes the contributions from the electronic and geometric changes, our energy decomposition analysis shows that even the steric effect favors the skew conformers, while the electronic and geometric changes stabilize the trans conformers. Thus, we conclude that both the hyperconjugative and steric interactions lower the energy of skew conformers and eventually form low barriers from skew to trans conformers and high barriers from skew to cis conformers in both $H_2O_2$ and $N_2H_4$. Comparison between the VB and the natural bond orbital (NBO) results show similarities and discrepancies between the two methods.

## Introduction

Internal rotations about single bonds, which play an important role in conformational analyses, have been well explored experimentally and theoretically, and the barriers are often elucidated in terms of electronic and steric effects.[1] Although a stringent separation of these two often competing effects is generally difficult, physical intuitions led to the repulsion model which states that, in most if not all cases, the repulsive Pauli exchange interactions dominate the rotation barriers.[2,3] Theoretically, however, the role of hyperconjugative interaction in internal rotations has been well recognized.[4,5] For instance, Mulliken even presented theoretical details to analyze the hyperconjugation in ethane soon after the barrier was experimentally determined (a historical review on ethane rotation barrier can be found in ref 6), but he also cautioned that the hyperconjugation in ethane is only of second order and "should have little or no direct effect in restricting free rotation".[4] The magnitude of hyperconjugation between two saturated groups was unknown until a few recent works particularly in the ethane case based on the natural bond orbital (NBO) method.[7−10] These works showed that it is the attractive $\sigma_{CH}$→$\sigma_{CH}$* hyperconjugative interactions be-

* Corresponding author phone: (269)387-2916; fax: (269)387-2909; e-mail: ymo@wmich.edu.
[†] Xiamen University.
[‡] Western Michigan University.

10.1021/ct049843x CCC: $30.25 
Published on Web 04/07/2005

***Chart 1***

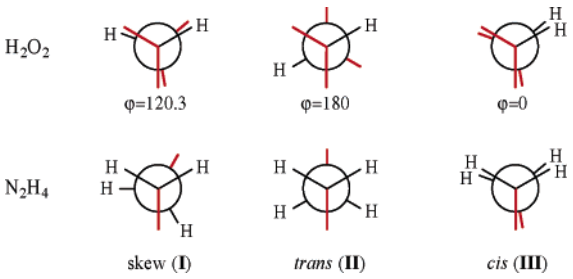


tween two methyl groups that stabilizes the staggered conformer. This hyperconjugation model even shows that the Pauli exchange energy actually stabilizes the eclipsed conformer of ethane relative to the staggered conformer.[10] In other words, the eclipsed structure would be preferred if hyperconjugative interactions were quenched. In contrast to the hyperconjugation model, most recently, two groups using very different methods consistently demonstrated that the steric hindrance dominates the ethane rotation barrier, although the hyperconjugative interaction does favor the staggered conformer.[11,12] However, we note that this controversy is not ended yet.[13] Arguably, this repulsion explanation for the ethane rotation barrier was supported by a recent finely designed experiment.[14]

Considering that the lone pair and antibond orbital (n→$\sigma$*) type of hyperconjugation should be more pronounced than the $\sigma$→$\sigma$* type due to the generally higher energy level for lone pairs than $\sigma$ bond electrons, we plan to use the modern ab initio valence bond (VB) method to probe the rotational barriers in hydrogen peroxide and hydrazine and examine the impact of the n→$\sigma$* negative hyperconjugation effect (or anomeric effect in the skew structures[15]) on the molecular energetics. The existence of n→$\sigma$* negative hyperconjugation as well as its influence on molecular structure and chemical reactivity have been well recognized both experimentally[16] and computationally.[17] Similarly, numerous computational studies have been conducted on hydrogen peroxide[18−21] and hydrazine.[20−22] Both computations and experiments[23,24] show that skew structures **I** (see Chart 1 where bold red lines represent lone pairs) in both systems are energy-minimum states with low barriers to trans (staggered) structures **II** but considerable barriers to cis (eclipsed) structures **III**. Notably, Smits and Altona used nonorthogonal and strictly localized molecular orbitals (MOs) and a single Slater determinant to study internal rotations for a few simple systems including $H_2O_2$ and $N_2H_4$.[25] Our goal in this paper is to employ the modern ab initio VB method to investigate the electronic and steric effects in these conformers and elucidate the driving forces for their torsional energy curves.

## Computational Methods

To delineate the electronic and steric effects, it is essential to remove the delocalization tails from molecular orbitals and derive the localized bond orbitals since the electronic effect, or more specifically the hyperconjugation effect involved in the rotation about a single bond, results from the interaction between occupied bond orbitals (e.g., $\sigma_{CH}$ in ethane) in one end and antibond orbitals (e.g., $\sigma_{CH}$*) in the other end of the single bond, which subsequently stabilizes the systems. The hyperconjugation energy is generally defined as the energy change owing to the mixture among the bond and antibond orbitals which leads to the delocalized orbitals.[26] However, in the MO theoretical calculations only delocalized orbitals can be obtained self-consistently. Assumptions have to be adopted to derive localized bond orbitals. If the latter are not optimal, the hyperconjugation energy might be significantly overestimated, and consequently the electronic effect will be biased against the steric effect in the analysis of the origin of conformational differences.[11,12] By using VB theory to construct both the localized (Lewis structure) and delocalized wave functions independently and self-consistently and compute the hyperconjugative stabilization explicitly in both the staggered and eclipsed structures of ethane and its congeners, we found that the steric strain dominates both rigid and fully relaxed rotations in all the group IVB ethane congeners, although the hyperconjugation effect does favor the staggered structures.[12,27]

Compared with the MO theory which interprets the electronic effect in terms of molecular orbital interactions, the VB theory is established on resonance structures, and thus a molecule is described by a set of resonance structures.[2,28] The electronic effect within the VB theory is measured by the magnitude of the contributions of certain ionic resonance structures to the most stable resonance structure (or Lewis structure as in the NBO method). Each resonance structure can be represented by a Heilter-London-Slater-Pauling (HLSP) function, which can be expanded into a linear combination of $2^m$ Slater determinants ($m$ is the number of covalent bonds in the target system) or by its equivalent spin-free form such as the bonded tableau are used in our approach,[29] or in a preferable form with bond orbitals as (hereby we assume the total spin quantum number $S = 0$)

$$\Phi_k = N_k\hat{A}(\phi_{1,2}\phi_{3,4}\cdots\phi_{2m-1,2m}) \tag{1}$$

where $\hat{A}$ is the antisymmetrizer, $N_k$ is the normalization constant, and $\phi_{i,j}$ is simply a bond function corresponding to the bond between orbitals $\varphi_i$ and $\varphi_j$

$$\phi_{i,j} = \hat{A}\{\varphi_i\varphi_j[\alpha(i)\beta(j) - \beta(i)\alpha(j)]\} \tag{2}$$

where the spins of electrons ($\alpha$ and $\beta$) are explicitly considered and both $\varphi_i$ and $\varphi_j$ are expanded in the basis functions on the two bonding atoms and called bond-distorted orbitals (BDOs).[30] Eq 2 shows that a bond orbital is not only a singlet spin eigenfunction but also comprised of two Slater determinants. The wave function for the molecule is expressed as a linear combination of all VB functions

$$\Psi = \sum_K C_K\Phi_K \tag{3}$$

Despite the fact that VB concepts are much more familiar to chemists and the VB theory was proposed earlier than the MO theory, currently the ab initio VB method lags far behind the MO methods due to the extremely high computational demand in the evaluation of overlap and the

Hamiltonian matrix elements among the VB functions. In comparison, the orthogonality restraint among MOs makes the MO-based methods extremely efficient. However, it should be emphasized that the MO and VB theories are supplementary and consistent rather than conflicting and competing.[31] During the past decade, modern ab initio VB methods have been developed with a few practical codes available.[32−35] Applications have distinctively demonstrated the importance of the VB approaches in gaining new insights into molecular structures, properties, and reactivity, which provide an understanding of the results obtained from the MO computations from a different perspective. In the quest for efficient algorithms in the ab initio VB computations, we introduced a new function called paired-permanent-determinant (PPD), which is an algebrant.[34] The introduction of PPD simplifies the CPU and memory requirements and an algorithm of 2 × (*N*-2) expansion is used in the present version of our code, XMVB.[35,36]

For hydrogen peroxide and hydrazine, initially we define the VB wave functions for their respective covalent resonance (or Lewis) structures as

$$\Phi_L(H_2O_2) = N_1\hat{A}(K_{O_1}K_{O_2}\sigma_{O_1H_1}\sigma_{O_2H_2}n_{1O_1}n_{2O_1}n_{1O_2}n_{2O_2}) \quad (4a)$$

$$\Phi_L(N_2H_4) = N_1\hat{A}(K_{N_1}K_{N_2}\sigma_{N_1H_1}\sigma_{N_1H_2}\sigma_{N_2H_3}\sigma_{N_2H_4}n_{N_1}n_{N_2}) \quad (4b)$$

where $K$ and $n$ refer to the core orbitals and lone pairs, respectively, and each bond orbital $\sigma_{ij}$ is a BDO localized on the two bonding atoms $i$ and $j$ only.[30] Obviously, a lone pair orbital is solely localized on one O or N atom. In principle, wave functions for ionic resonance structures can be written out similarly, and the simultaneous optimization of the orbitals and configuration coefficients results in the overall wave function $\Psi$ as shown in eq 3. However, the most significant feature of modern ab initio VB methods is the flexibility of the one-electron orbitals that are allowed to expand and optimize either in the full space of basis functions of the system or in its subspaces.[30,33] The use of delocalized overlap-enhanced orbitals (OEOs),[37] which are expanded in the whole molecular space much like regular MOs, provides the key to the construction of VB functions of considerable accuracy and compactness. Since normally neutral resonance structures are much more stable than ionic resonance structures, using OEOs and only neutral covalent structures can recover the electron correlations overwhelmingly. E.g., for benzene Cooper et al. have demonstrated that over 93% of electron correlation can be recovered by adopting two Kékule and three Dewar structures.[38] For the current cases of hydrogen peroxide and hydrazine, ionic structures are clearly unfavorable, and high energy gaps between the stable covalent structure and the unstable ionic structures are anticipated since $\sigma$ bonds usually cost much more energy to break than $\pi$ bonds. Thus, we skip the ionic structures by using delocalized OEOs and define the wave function for $H_2O_2$ and $N_2H_4$ as

$$\Psi(H_2O_2) = N'\hat{A}(K_{O_1}K_{O_2}\sigma_{O_1H_1}'\sigma_{O_2H_2}'n_{1O_1}'n_{2O_1}'n_{1O_2}'n_{2O_2}') \quad (5a)$$

$$\Psi(N_2H_4) = N'\hat{A}(K_{N_1}K_{N_2}\sigma_{N_1H_1}'\sigma_{N_1H_2}'\sigma_{N_2H_3}'\sigma_{N_2H_4}'n_{N_1}'n_{N_2}') \quad (5b)$$

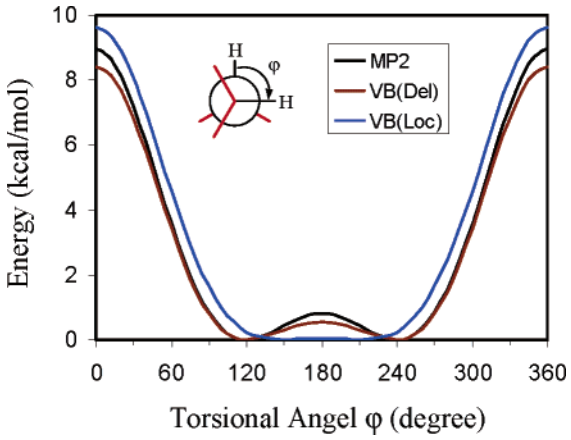


***Figure 1.*** Comparison of energy profiles for the hydrogen peroxide rotation where the hyperconjugation effect is considered (black and brown lines) or screened out (blue line).

where the orbital $\sigma_{ij}'$ contains $\varphi_i'$ and $\varphi_j'$ like eq 2, but the latter are expanded in the whole basis space of the molecule, rather than the subspace of two bonding atoms as $\varphi_i$ and $\varphi_j$ in $\Phi_L$. Similarly, $\{n'\}$ are delocalized over the whole molecule too. Once the localized and delocalized wave functions are defined as in eqs 4 and 5, the hyperconjugative stabilization energy $E_{hc}$ can be estimated as the energy difference between them

$$E_{hc} = E(\Psi) - E(\Phi_L) = \langle\Psi|\hat{H}|\Psi\rangle - \langle\Phi_L|\hat{H}|\Phi_L\rangle \quad (6)$$

where $\hat{H}$ is the Hamiltonian operator. It should be pointed out that both $\Psi$ and $\Phi_L$ can be expanded into $2^2 = 4$ Slater determinants for hydrogen peroxide and $2^4 = 16$ Slater determinants for hydrazine, and in our code all orbitals in eqs 4 and 5 are optimized self-consistently.

To fully examine the hyperconjugative interactions in hydrogen peroxide and hydrazine along the rotational trajectories, geometries are fully optimized at each torsional angle at the MP2/6-311G(d,p) (6D) level, followed by the VB calculations with the same basis set. MP2 geometry optimizations as well as the primitive integrals that are required for VB calculations were carried out using Gaussian98,[39] while VB calculations were performed with our XMVB program.[35]

## Results and Discussion

**Torsional Potential Energy Surfaces (PESs).** Figures 1 and 2 plot the energy profiles (black and brown curves) arising from internal rotations about the central O−O bond in $H_2O_2$ and the N−N bond in $N_2H_4$, respectively. Relative energies of the energy minimum and maximum conformers from the MP2 and VB calculations are compiled and compared with the experimental data in Table 1. Both systems have similar PESs and two energetically favored rotational positions, thus the internal rotations are hindered. In both molecules, skew conformers are the energy-minimum states and even more stable than the trans conformers which may have the least steric repulsion between the two OH or $NH_2$ moieties from the perspective of the simple repulsion model. However, the barriers from skew to trans conformers are slightly under-

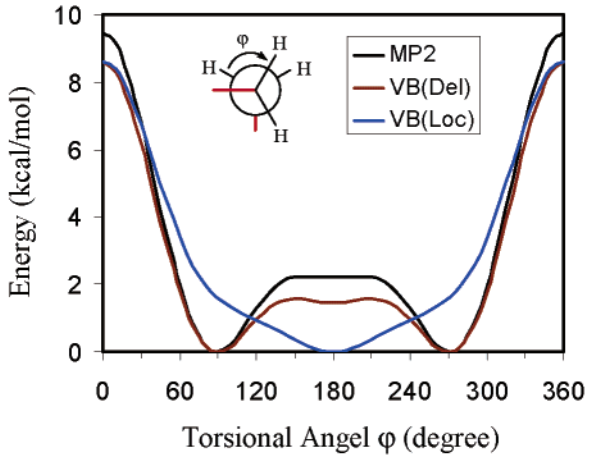


***Figure 2.*** Comparison of energy profiles for the hydrazine rotation where the hyperconjugation effect is considered (black and brown lines) or screened out (blue line).

***Table 1.*** Comparison of Relative Energies (Rotational Barriers) with the MP2 and VB Methods and 6-311G(d,p) Basis Set (kcal/mol)

| molecule | $\varphi$ (°) | conformer | $\Delta E_{rot}$(MP2) | $\Delta E_{rot}$(VB) | $\Delta E_{rot}$(expt) |
|---|---|---|---|---|---|
| $H_2O_2$ | 120.1 | skew ($C_2$) | 0.0 | 0.0 | 0.0 |
| | 180.0 | trans ($C_{2h}$) | 0.82 | 0.54 | 1.11[a] |
| | 0.0 | cis ($C_{2v}$) | 8.95 | 8.42 | 7.33[a] |
| $N_2H_4$ | 89.1 | skew ($C_2$) | 0.0 | 0.0 | 0.0 |
| | 180.0 | trans ($C_2$) | 2.21 | 1.46 | 3.14[b] |
| | 0.0 | cis ($C_{2v}$) | 9.48 | 8.61 | |

[a] Reference 40. [b] Reference 24.

estimated at both the MP2/6-311G(d,p) and VB/6-311G(d,p) levels compared with high-level computations as well as experimental data. E.g., Chung-Phillips and Jebber obtained 1.20 and 3.27 kcal/mol at the MP2/6-311+G(3df,2p) level for $H_2O_2$ and $N_2H_4$,[21] while Halpern and Glendening derived a value of 1.04 kcal/mol for $H_2O_2$ at the CCSD(T)/CBS level.[19] The far-IR spectrum yields a trans barrier of 1.10 kcal/mol for $H_2O_2$[40] and 3.14 kcal/mol for $N_2H_4$[24]. These results are in contrast to their isoelectronic system ethane, which favors the trans conformer as the energy-minimum state, and no stable skew conformer is found. Obviously, the discrepancy comes from the involvement of lone pairs in $H_2O_2$ and $N_2H_4$, whose exact role will be investigated in the next sections.

Compared with ethane, both $H_2O_2$ and $N_2H_4$ have a much higher rotational barrier from the energy-minimum state to the cis conformer, and our data are 8.41 and 8.60 kcal/mol which are comparable to 7.79 and 8.96 kcal/mol at the MP2/6-311+G(3df,2p) level for $H_2O_2$ and $N_2H_4$.[21] The CCSD(T)/CBS level leads to a barrier of 7.13 kcal/mol for $H_2O_2$[19] in agreement with the experimental value of 7.33 kcal/mol.[40]

Depicted also in Figures 1 and 2 are the torsional energy profiles (blue curves) of the Lewis structures (eq 4) where the hyperconjugative interactions are quenched. Thus, the energy profiles of $\Phi_L$ mostly correspond to effects due to the Pauli exchange and electrostatic repulsion interactions or steric effects. The structural effect which mainly concerns the change of the central bond lengths may also be involved

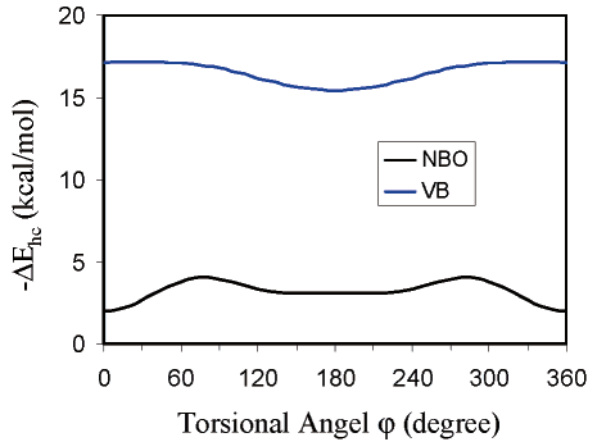


***Figure 3.*** Comparison of the hyperconjugation effect during the hydrogen peroxide ($H_2O_2$) rotation estimated by the NBO method (black line) and VB method (blue line).

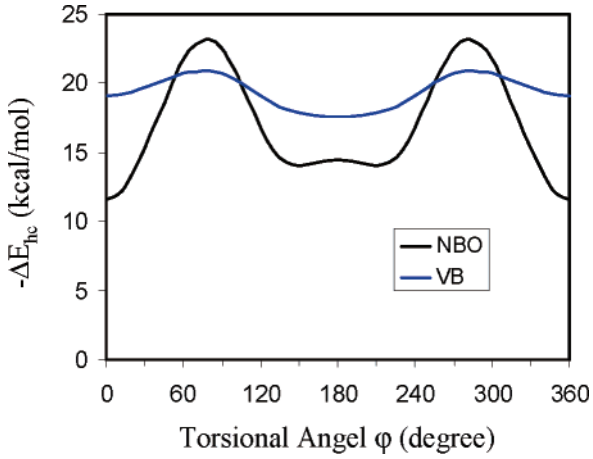


***Figure 4.*** Comparison of the hyperconjugation effect during the hydrazine ($N_2H_4$) rotation estimated by the NBO method (black line) and VB method (blue line).

in the energy curves of Lewis structures and will be elaborately explored in the following. Much similar to ethane, our results demonstrate that when hyperconjugative interactions in $H_2O_2$ and $N_2H_4$ are excluded, the trans conformers are favored over the cis conformers by 9.62 and 8.62 kcal/mol, while the minimums at the skew conformers disappear in the potential energy surfaces pertaining to torsional motions. These findings once again confirmed that it is the lone pairs that complicate the overall torsional potential energy surfaces of $H_2O_2$ and $N_2H_4$.

**Hyperconjugative Interaction.** Since our focus in this work is the relative contributions of the hyperconjugation and steric effects to the torsional energy profiles, we performed ab initio VB calculations with the 6-311G(d,p) basis set where the one-electron orbitals are either delocalized OEOs (eq 5) or bond-localized BDOs (eq 4), and the hyperconjugation energy is derived with eq 6. For comparison hyperconjugation energies are also computed with the NBO method at the HF level. Figures 3 and 4 showed the variation of the VB and NBO hyperconjugation energies with respect to the torsional angle. The NBO delocalization energies are computed based on the deletion of off-diagonal elements between X−H bond orbitals and lone pair(s) on X

***Table 2.*** Hyperconjugation Energies (kcal/mol) in $H_2O_2$ and $N_2H_4$ with the ab Initio VB Method and NBO Method at the MP2/6-311G(d,p) Optimal Geometries

| molecule | conformer | $E(\Psi)$ (au) | $E(\Phi_L)$ (au) | $E_{hc}$ (VB) | $E_{hc}$ (NBO) |
|---|---|---|---|---|---|
| $H_2O_2$ | skew ($C_2$) | −150.90545 | −150.87967 | −16.18 | −3.32 |
| | trans ($C_{2h}$) | −150.90459 | −150.88000 | −15.43 | −3.13 |
| | cis ($C_{2v}$) | −150.89204 | −150.86472 | −17.14 | −2.02 |
| $N_2H_4$ | skew ($C_2$) | −111.30849 | −111.27550 | −20.70 | −22.57 |
| | trans ($C_2$) | −111.30617 | −111.27807 | −17.63 | −14.47 |
| | cis ($C_{2v}$) | −111.29478 | −111.26434 | −19.10 | −11.55 |

(X = O, N) in one moiety and X−H antibond orbitals in the other moiety. A total of 6 elements for $H_2O_2$ and 12 elements for $N_2H_4$ are deleted. Table 2 listed the VB total energies and the subsequent VB hyperconjugation energies as well as the NBO hyperconjugation energies for the skew, trans, and cis conformers.

The comparison of the VB and NBO hyperconjugation energies reveals some interesting similarities and differences between the two methods. Both methods result in similar fluctuation patterns of the hyperconjugation energies with respect to the torsional angle, e.g., at the torsional angle around 80°, the hyperconjugative interactions reach the maximum, although the VB calculations result in a very flat plateau in the range of $\varphi = 0°-80°$ (and 280°−360°) for $H_2O_2$, while the NBO method leads to a decreasing of the hyperconjugative interaction with the reduction of the torsional angel from 80°, and the cis conformer of $H_2O_2$ has the weakest hyperconjugation effect. Nevertheless, both VB and NBO agree that the trans conformers of $H_2O_2$ and $N_2H_4$ have weaker hyperconjugative interaction than the skew conformers, strongly indicating that the preference of the skew conformer over the trans conformers is at least partially contributed by the favorable hyperconjugative stabilization in the formers. Although the VB and NBO hyperconjugation energies have a comparable fluctuation magnitude (around 2 kcal/mol), a huge discrepancy is observed in their absolute values (Figure 3). In the VB calculations, part of the hyperconjugation energies actually should be ascribed to the geminal bond−antibond interactions between OH or $NH_2$ groups and the O−O or N−N bond and antibond, which has been discussed in the previous works[12,27] and first pointed out by Reed and Weinhold.[9] These geminal interactions are essentially invariable with respect to internal rotation due to symmetry, and thus only the difference among various conformers is the focal point in our current investigation of the nature of rotational barriers. However, a similar computational strategy showed that the VB and NBO hyperconjugation energies are of the same magnitude in $N_2H_4$, although the NBO data now fluctuate significantly compared with the VB data. Comparably, in the isoelectronic system $C_2H_6$, the NBO hyperconjugation energies in the staggered and eclipsed structures are −24.88 and −18.36 kcal/mol, whereas the VB data are −13.1 and −12.1 kcal/mol. Based on the VB calculations, we found that the overall hyperconjugation effect between two groups connected by the central single bond increases in the order of $C_2H_6 < H_2O_2 < N_2H_4$. This order may suggest that the n→$\sigma$* negative hyperconjugation effect is stronger than the $\sigma$→$\sigma$* hyperconjugation effect. For the same type n→$\sigma$* or $\sigma$→$\sigma$* interactions, however, the effect weakens with the increasing of the electronegativity of the X atom in the $\sigma_{XH}$ or $\sigma_{XH}$*.

Typically, for the sake of simplicity we assume that the rotational barriers are composed of steric and hyperconjugative energy terms, and the steric energy is thus simply taken as the difference between the overall rotational barriers and hyperconjugative energies which are shown in Tables 1 and 2 and plotted in Figures 1−4. On the basis of this approach, both the VB and NBO methods predict negligible energy changes around the trans conformer of $H_2O_2$ ($\varphi$ = 120°−240°), and the cis conformer would be the energy-maximum state, if there were no hyperconjugation effect. Disagreement between the VB and the NBO methods shows up in the $N_2H_4$ case, where the VB method consistently predicts an energy peak at the cis conformer as already demonstrated by the energy curve of the Lewis structure in Figure 2, but the NBO method favors the skew structure as the energy-maximum state, while the cis conformer is a local minimum in the steric energy profile.

Interestingly, it is clear that the hyperconjugation effect is not solely dominated by single n→$\sigma$* negative hyperconjugative effect as otherwise the following conformers would be preferred as one lone pair is in a perfect antiparallel position ($\varphi$ = 60°) with a X−H bond, as there is a better overlap between the lone pair orbital and $\sigma_{XH}$* (X = O or N).

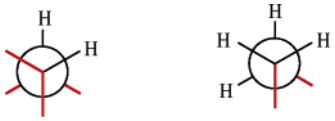


**Steric Hindrance and Structural Effect.** Although in the above we assumed that the rotational barrier comes from the attractive electronic effect (hyperconjugation) and the repulsion steric effect and the steric effect can be estimated by subtracting the hyperconjugation energy from the overall rotational barrier, it is desirable to evaluate the steric energy independently. Moreover, some recent studies supporting the attractive explanation for rotation heights around single bonds also showed that the interpretation of the barrier is influenced by the slight change of the central bond. In other words, rigid rotations and relaxed rotations albeit that they have very close barriers could have very different rotation mechanisms.[8,10,41] Thus, it is illuminating to discern the electronic and geometric relaxations, particularly in the central O−O or N−N bond, in the process of rotations. In the simple treatment, these effects are usually merged into the steric effect. In the analysis on ethane and its congeners, we proposed a solution to probe the energetic variation by freezing the bond orbitals $\{\phi_{i,j}\}$ during the rotation when the hyperconjugation effect is deactivated.[12,27] As a consequence, the steric repulsion and electronic and geometric relaxations can be individually enumerated as the molecule undergoes changes from one conformer to others.

Here we adopted the above strategy to systematically explore the hyperconjugation, steric, structural relaxation, and electronic relaxation effects in the rotation. Taking the skew

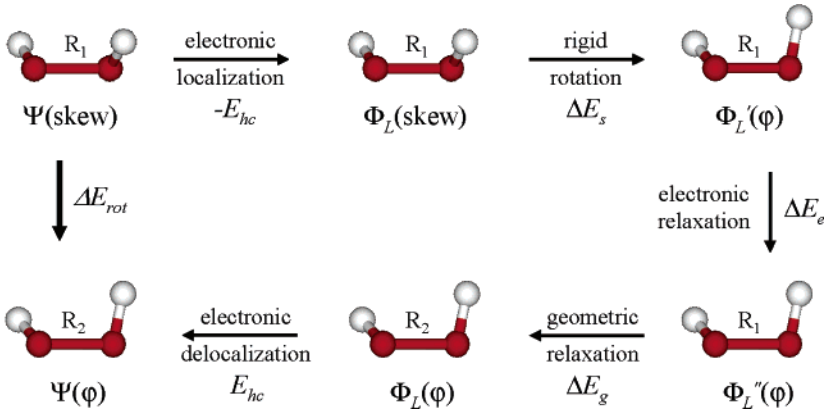


***Figure 5.*** A stepwise decomposition scheme to explore the geometric impact on the rotation barrier in hydrogen peroxide.

conformers as references, we decompose the overall rotational process into the following five successive steps as shown in Figure 5: (1) At the optimal geometry of the skew conformer of $H_2O_2$ or $N_2H_4$, deactivate the hyperconjugation effect. The energy variation in this step is the reverse of the hyperconjugation energy defined by eq 6 in the skew conformer ($-E_{hc} = 16.18$ for $H_2O_2$ or 20.70 kcal/mol for $N_2H_4$ as listed in Table 2). (2) Freeze all orbitals and structural parameters except the dihedral angle $\varphi$, rotate one OH or $NH_2$ group by a certain amount, and recompute the total energy by fixing all bond orbitals without any SCF calculations. In this step, a Jacobi $2 \times 2$ matrix transformation is applied to the *p* and *d* orbitals of the rotated OH or $NH_2$ group. Energy changes ($\Delta E_s$) in this step come from the steric repulsion in the rigid rotation as no other factors are involved except from the Pauli repulsion and electrostatic interactions between the two adjacent groups. (3) Relax the frozen orbitals in the above step. The reoptimization (relaxation) of the bond orbitals inherited from the skew conformer will stabilize the rotated structure by $\Delta E_e$, and we define this step as the electronic relaxation step. (4) Relax the geometry to the optimal rotated structure at this torsional angle $\varphi$. The geometric change is dominated by the variation of the central bond and the accompanied energy reduction ($\Delta E_g$) results from the structural effect. (5) Delocalize the electrons between the two OH or $NH_2$ groups which is the hyperconjugation effect in the rotated structure and the energy change is $E_{hc}(\varphi)$. After summing up all the above five energy terms, the overall energy change by transforming the structures of $H_2O_2$ and $N_2H_4$ from the skew conformer to a rotated conformer with torsional angle $\varphi$ is

$$\Delta E_{rot} = -E_{hc}(\text{skew}) + \Delta E_s + \Delta E_e + \Delta E_g + E_{hc}(\varphi)$$
$$= \Delta E_{hc} + \Delta E_s + \Delta E_e + \Delta E_g \qquad (7)$$

Figures 6 and 7 show the changes of various energy terms in eq 7 with respect to the torsional angle $\varphi$ and values for skew, trans, and cis conformers are collected in Table 3. On the basis of the above energy decomposition, we found that unlike the cases of ethane and its congeners,[12,27] both electronic and geometric relaxations make noticeable energy changes in the rotation, although the overall energy curve is solely dominated by the steric effect. However, since the changes from skew to trans conformers require much less energy than the skew→cis rotations, we found that actually the steric effect does not favor the trans conformers. Rather, it is the electronic and structural relaxations that stabilize the trans conformers and make the trans conformers as the energy-minimum states when the hyperconjugation effect is

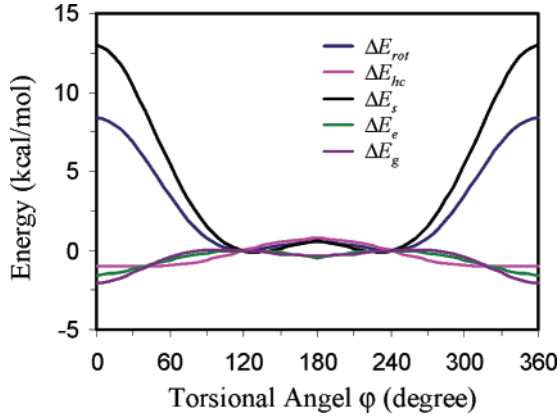


***Figure 6.*** Decomposition of the rotational energy ($\Delta E_{rot}$) in terms of hyperconjugation effect ($\Delta E_{hc}$), steric repulsion ($\Delta E_s$), electronic relaxation ($\Delta E_e$), and geometric relaxation ($\Delta E_g$) for hydrogen peroxide.

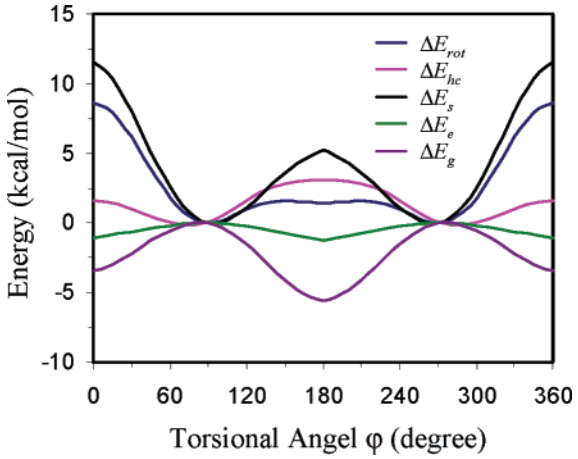


***Figure 7.*** Decomposition of the rotational energy ($\Delta E_{rot}$) in terms of hyperconjugation effect ($\Delta E_{hc}$), steric repulsion ($\Delta E_s$), electronic relaxation ($\Delta E_e$), and geometric relaxation ($\Delta E_g$) for hydrazine.

***Table 3.*** Energy Decomposition of the Rotational Barriers in Terms of Hyperconjugation, Steric, Electronic Relaxation, and Geometric Relaxation Effects (kcal/mol)

| | skew → cis | | | | | skew → trans | | | | |
|---|---|---|---|---|---|---|---|---|---|---|
| molecule | $\Delta E_{rot}$ | $\Delta E_{hc}$ | $\Delta E_s$ | $\Delta E_e$ | $\Delta E_g$ | $\Delta E_{rot}$ | $\Delta E_{hc}$ | $\Delta E_s$ | $\Delta E_e$ | $\Delta E_g$ |
| $H_2O_2$ | 8.42 | −0.96 | 13.01 | −1.59 | −2.04 | 0.54 | 0.75 | 0.61 | −0.45 | −0.37 |
| $N_2H_4$ | 8.61 | 1.60 | 11.52 | −1.08 | −3.43 | 1.46 | 3.07 | 5.20 | −1.25 | −5.56 |

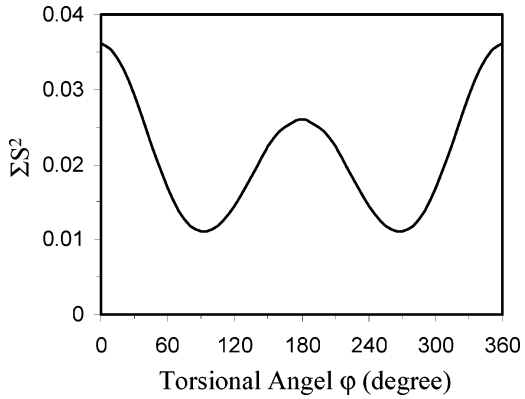


***Figure 8.*** Fluctuation of the sum of squares of overlap integrals among the oxygen lone pairs in hydrogen peroxide with respect to the torsional angle.

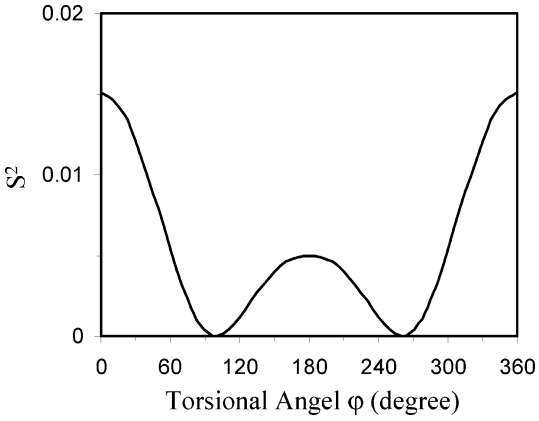


***Figure 9.*** Fluctuation of the square of the overlap integral between the nitrogen lone pairs in hydrazine with respect to the torsional angle.

deactivated. This finding is echoed by the variation of the sum of the squares of the overlap integrals among the lone pairs in the VB wave function of Lewis structures which can roughly measure the Pauli repulsion among the lone pairs in $H_2O_2$ and $N_2H_4$ (see Figures 8 and 9).[42] Interesting, Figures 8 and 9 have similar shapes to the torsional potential energy curves, indicating the repulsion among the lone pairs dominate the torsional energies. However, we must remember that when the rotational barriers are small, the electronic and geometrical relaxation may be involved and make the simple binary theory of hyperconjugation and steric repulsion not work well.

Figures 6 and 7 also reveal that the structural changes during the rotation have a much more significant impact on the energetics of $N_2H_4$ than that of $H_2O_2$. This is inconsistent with the much larger central bond lengthening in $N_2H_4$ than in $H_2O_2$. For instance, the MP2/6-311G(d,p) optimizations show that the N−N bond lengthens by 0.043 Å and 0.037 Å from the skew to the trans and cis conformers in $N_2H_4$, compared with only 0.009 Å and 0.006 Å for the O−O bond in $H_2O_2$.

## Conclusion

Ab initio VB calculations and subsequent analyses indicate that the preference of the skew conformers of hydrogen peroxide and hydrazine over both the trans and cis conformers comes from enhanced attractive hyperconjugative interactions and reduced repulsive steric interactions between the two bonding OH or $NH_2$ groups. Although the quenching of the hyperconjugation effect leads to the stabilization of the trans conformers as energy minimum states and the disappearance of the skew conformers in the torsional potential energy surfaces, it is the remarkable electronic and geometric relaxations rather than the steric hindrances that contribute to this interesting feature. In contrast to $H_2O_2$ and $N_2H_4$, ethane and its congeners show little electronic relaxations and small geometric relaxations.[23] Although conventionally it is approximated that rotational barriers are comprised of electronic and steric contributions, when the barriers are small or there are noticeable structural changes, it is pivotal to separate the structural relaxation contribution from the steric repulsion and estimate all energy terms individually. Our complete ab initio VB analyses demonstrate that the steric energies in $H_2O_2$ and $N_2H_4$ follow the same trends as the overall rotational barriers and show double well curves. It is also evident that the steric strain is dominated by the repulsion among the lone electron pairs on oxygen atoms in $H_2O_2$ and nitrogen atoms in $N_2H_4$, as the overlap integrals among the lone pair orbitals reveals the exact same fluctuation patterns.

**Acknowledgment.** The research at XMU is supported by the Natural Science Foundation of China (Grant Nos. 20225311, 20373052, and 20021002). Support from the Western Michigan University is also gratefully acknowledged (Y.M.).

### References

(1) Payne, P. W.; Allen, L. C. In *Modern Theoretical Chemistry*; Schaefer H. F., III, Ed.; Plenum Press: New York and London, 1977; Vol. 4, pp 29. Wiberg, K. B. In *Encyclopedia of Computational Chemistry*; Schleyer, P. v. R., Ed.; John Wiley & Sons: Berlin, 1998; p 2518.

(2) Pauling, L. C. *The Nature of the Chemical Bond*, 3rd ed.; Cornell University Press: Ithaca, NY, 1960.

(3) Sovers, O. J.; Kern, C. W.; Pitzer, R. M.; Karplus, M. *J. Chem. Phys.* **1968**, *49*, 2592. Hoyland, J. R. *J. Am. Chem. Soc.* **1968**, *90*, 2227.

(4) Mulliken, R. S. *J. Chem. Phys.* **1939**, *7*, 339.

(5) Lowe, J. *J. Am. Chem. Soc.* **1970**, *92*, 3799. England, W.; Gordon, M. S. *J. Am. Chem. Soc.* **1971**, *93*, 4649. Epiotis, N. D.; Cherry, W. R.; Shaik, S.; Yates, R. L.; Bernardi, F. *Topics in Current Chemistry: Structural Theory of Organic Chemistry*; 1977; Vol. 70.

(6) Schreiner, P. R. *Angew. Chem., Int. Ed.* **2002**, *41*, 3579.

(7) Brunck, T. K.; Weinhold, F. *J. Am. Chem. Soc.* **1979**, *101*, 1700. Reed, A. E.; Curtiss, L. A.; Weinhold, F. *Chem. Rev.* **1988**, *88*, 899. Goodman, L.; Gu, H. *J. Chem. Phys.* **1998**, *109*, 72. Goodman, L.; Gu, H.; Pophristic, V. *J. Chem. Phys.* **1999**, *110*, 4268. Goodman, L.; Pophristic, V.; Weinhold, F. *Acc. Chem. Res.* **1999**, *32*, 983.

(8) Corcoran, C. T.; Weinhold, F. *J. Chem. Phys.* **1980**, *72*, 2866.

(9) Reed, A. E.; Weinhold, F. *Isr. J. Chem.* **1991**, *31*, 277.

(10) Pophristic, V.; Goodman, L. *Nature* **2001**, *411*, 565.

(11) Bickelhaupt, F. M.; Baerends, E. J. *Angew. Chem., Int. Ed.* **2003**, *42*, 4183.

(12) Mo, Y.; Wu, W.; Song, L.; Lin, M.; Zhang, Q.; Gao, J. *Angew. Chem., Int. Ed.* **2004**, *43*, 1986.

(13) Weinhold, F. *Angew. Chem., Int. Ed.* **2003**, *42*, 4188.

(14) Bohn, R. K. *J. Phys. Chem. A* **2004**, *108*, 6814.

(15) Kirby, A. J. *The Anomeric Effect and Related Stereoelectronic Effects at Oxygen*; Springer: Berlin, 1983. Deslongchamps, P. *Stereoelectronic Effects in Organic Chemistry*; Pergamon: Oxford, 1983. *The Anomeric Effect and Associated Stereoelectronic Effects*; Thatcher, G. R., Ed.; American Chemical Society: Washington, DC, 1993.

(16) Raban, M.; Kost, D. *J. Am. Chem. Soc.* **1972**, *94*, 3234. Forsyth, D. A.; Yang, J. R. *J. Am. Chem. Soc.* **1986**, *108*, 2157. Kluger, R.; Brandl, M. *J. Org. Chem.* **1986**, *51*, 3964. Rahman, M. M.; Lemal, D. M.; Dailey, W. P. *J. Am. Chem. Soc.* **1988**, *110*, 1964. King, J. F.; Rathore, R.; Guo, Z.; Li, M.; Payne, N. C. *J. Am. Chem. Soc* **2000**, *122*, 10308. King, J. F.; Li, M.; Cheng, A. Z.; Dave, V.; Payne, N. C. *Can. J. Chem.* **2003**, *81*, 638. Hetenyi, A.; Martinek, T. A.; Lazar, L.; Zalan, Z.; Fueloep, F. *J. Org. Chem.* **2003**, *68*, 5705. Hoge, B.; Thosen, C.; Herrmann, T.; Pantenburg, I. *Inorg. Chem.* **2003**, *42*, 3633. Bansal, R. K.; Gupta, N.; Singh, S.; Karaghiosoff, K.; Mayer, P.; Vogt, M. *Tetrahedron Lett.* **2004**, *45*, 7771.

(17) Reed, A. E.; Schleyer, P. v. R. *J. Am. Chem. Soc.* **1990**, *112*, 1434. Wiberg, K. B.; Rablen, P. R. *J. Am. Chem. Soc.* **1993**, *115*, 614. Schneider, W. F.; Nance, B. I.; Wallington, T. J. *J. Am. Chem. Soc.* **1995**, *117*, 478. Raabe, G.; Gais, H.-J.; Fleischhauer, J. *J. Am. Chem. Soc.* **1996**, *118*, 4622. Mo, Y.; Zhang, Y.; Gao, J. *J. Am. Chem. Soc.* **1999**, *121*, 5737. Scherer, W.; Sirsch, P.; Shorokhov, D.; McGrady, G. S.; Mason, S. A.; Gardiner, M. G. *Euro. J. Chem.* **2002**, *8*, 2324. Kormos, B. L.; Cramer, C. J. *Inorg. Chem.* **2003**, *42*, 6691. Lill, S. O. N.; Rauhut, G.; Anders, E. *Chem.: Euro. J.* **2003**, *9*, 3143.

(18) Fink, W. H.; Allen, L. C. *J. Chem. Phys.* **1967**, *46*, 2261. Davidson, R. B.; Allen, L. C. *J. Chem. Phys.* **1971**, *55*, 519. Dunning, T. H., Jr.; Winter, N. W. *J. Chem. Phys.* **1975**, *63*. Christiansen, P. A.; Palke, W. E. *J. Chem. Phys.* **1977**, *67*, 57. Howard, R. E.; Levy, M.; Shull, H.; Hagstrom, S. *J. Chem. Phys.* **1977**, *66*, 5189. Rodwell, W. R.; Carlsen, N. R.; Radom, L. *Chem. Phys.* **1978**, *31*, 177. Cremer, D. *J. Chem. Phys.* **1978**, *69*, 4440. Block, R.; Jansen, L. *J. Chem. Phys.* **1985**, *82*, 3322.

(19) Halpern, A. M.; Glendening, E. D. *J. Chem. Phys.* **2004**, *121*, 273.

(20) Pedersen, L.; Morokuma, K. *J. Chem. Phys.* **1967**, *46*, 3941. Lombardi, E.; Tarantini, G.; Pirola, L.; Torsellini, P. *J. Chem. Phys.* **1976**, *64*, 5229.

(21) Chung-Phillips, A.; Jebber, K. A. *J. Chem. Phys.* **2001**, *102*, 7080.

(22) Fink, W. H.; Pan, D. C.; Allen, L. C. *J. Chem. Phys.* **1967**, *47*, 895. Wagner, E. L. *Theor. Chim. Acta* **1971**, *23*, 115. Grana, A. M.; Mosquera, R. A. *J. Mol. Struct.* **2000**, *556*, 69.

(23) Hunt, R. H.; Leacock, R. A.; Peters, C. W.; Hecht, K. T. *J. Chem. Phys.* **1965**, *42*, 1931.

(24) Kasuya, T.; Kojima, T. *J. Phys. Soc. Jpn.* **1963**, *18*, 364.

(25) Gordon, M. S. *J. Am. Chem. Soc.* **1969**, *91*, 3122. Smits, G. F.; Altona, C. *Theor. Chim. Acta* **1986**, *67*, 461. Smits, G. F.; Krol, M. C.; Altona, C. *Mol. Phys.* **1988**, *63*, 921.

(26) Cramer, C. J. In *Encyclopedia of Computational Chemistry*; Schelyer, P. v. R., Ed.; John Wiley & Sons: Berlin, 1998; p 1294.

(27) Song, L.; Lin, Y.; Wu, W.; Zhang, Q.; Mo, Y. *J. Phys. Chem. A* **2005**, *ASAP, DOI: 10.1021/jp044700s*.

(28) Wheland, G. W. *Resonance in Organic Chemistry*; Wiley: New York, 1955.

(29) Li, X.; Zhang, Q. *Int. J. Quantum Chem.* **1989**, *36*, 599. Zhang, Q.; Li, X. *J. Mol. Struct.* **1989**, *189*, 413. Wu, W.; Mo, Y.; Cao, Z.; Zhang, Q. In *Valence Bond Theory*; Cooper, D. L., Ed.; Elsevier: Amsterdam, 2002; Vol. 10, p 143.

(30) Mo, Y.; Lin, Z.; Wu, W.; Zhang, Q. *J. Phys. Chem.* **1996**, *100*, 11569.

(31) Hoffman, R.; Shaik, S.; Hiberty, P. C. *Acc. Chem. Res.* **2003**, *36*, 750.

(32) *Valence Bond Theory*; Cooper, D. L., Ed.; Elsevier: Amsterdam, 2002. Mcweeny, R. *Int. J. Quantum Chem.* **1999**, *74*, 87. Dijkstra, F.; van Lenthe, J. H. *J. Chem. Phys.* **2000**, *113*, 2100. Thorsteinsson, T.; Cooper, D. L. *J. Math. Chem.* **1998**, *23*, 105.

(33) Cooper, D. L.; Gerratt, J.; Raimondi, M. *Chem. Rev.* **1991**, *91*, 929. Hiberty, P. C. *THEOCHEM* **1997**, *398*−*399*, 35.

(34) Wu, W.; Wu, A.; Mo, Y.; Lin, M.; Zhang, Q. *Int. J. Quantum Chem.* **1998**, *67*, 287.

(35) Wu, W.; Song, L.; Mo, Y.; Zhang, Q. XMVB - An ab initio spin-free valence bond (VB) program; Xiamen University, Xiamen, China, 2000.

(36) Song, L.; Mo, Y.; Zhang, Q.; Wu, W. *J. Comput. Chem.* **2005**, 26, 514.

(37) Coulson, C. A.; Fischer, I. *Philos. Mag.* **1949**, *40*, 386.

(38) Cooper, D. L.; Gerratt, J.; Raimondi, M. *Nature* **1986**, *323*, 699.

(39) Frisch, M. J.; Trucks, G. W.; Schlegel, H. B.; Scuseria, G. E.; Robb, M. A.; Cheeseman, J. R.; Zakrzewski, V. G.; Montgomery, J. A. J.; Stratmann, R. E.; Burant, J. C.; Dapprich, S.; Millam, J. M.; Daniels, A. D.; Kudin, K. N.; Strain, M. C.; Farkas, O.; Tomasi, J.; Barone, V.; Cossi, M.; Cammi, R.; Mennucci, B.; Pomelli, C.; Adamo, C.; Clifford, S.; Ochterski, J.; Petersson, G. A.; Ayala, P. Y.; Cui, Q.; Morokuma, K.; Malick, D. K.; Rabuck, A. D.; Raghavachari,

K.; Foresman, J. B.; Cioslowski, J.; Ortiz, J. V.; Baboul, A. G.; Stefanov, B. B.; Liu, G.; Liashenko, A.; Piskorz, P.; Komaromi, I.; Gomperts, R.; Martin, R. L.; Fox, D. J.; Keith, T.; Al-Laham, M. A.; Peng, C. Y.; Nanayakkara, A.; Challacombe, M.; Gill, P. M. W.; Johnson, B.; Chen, W.; Wong, M. W.; Andres, J. L.; Gonzalez, C.; Head-Gordon, M.; Replogle, E. S.; Pople, J. A. A.9 ed.; Gaussian, Inc.: Pittsburgh, PA, 1998.

(40) Flaud, J. M.; Camy-Peyret, C.; Johns, J. W. C.; Carli, B. *J. Chem. Phys.* **1989**, *91*, 1504.

(41) Bader, R. F. W.; Cheeseman, J. R.; Laidig, K. E.; Wiberg, K. B.; Breneman, C. *J. Am. Chem. Soc.* **1990**, *112*, 6530. Pophristic, V.; Goodman, L.; Wu, C. T. *J. Phys. Chem. A* **2001**, *105*, 7454.

(42) The exchange integral between two doubly occupied orbitals can be approximated as $(ij|ij) = (1/4)S_{ij}^2[(ii|ii) + 2(ii|jj) + (jj|jj)]$. See: Murrell, J. N.; Harget, A. J. *Semiempirical Self-Consistent-Field Molecular Orbital Theory of Molecules*; Wiley-Interscience: London, 1972; p 147.

CT049843X